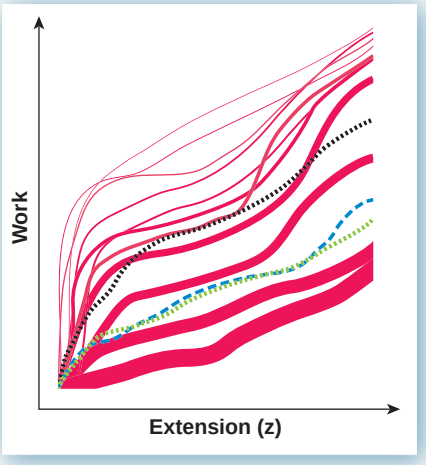


**Unfolding an RNA molecule.** This figure is schematic and not based on real data. Dashed blue line: free energy as a function of extension $z$ from the reversible work. Solid red curves: many different trials of unfolding at nonequilibrium rates; line thicknesses represent the relative weightings necessary to satisfy Jarzynski's equality. Dotted green line: free energy determined with Jarzynski's equality. Dotted black line: equally weighted average of the nonequilibrium work.

of the work measured for many repetitions of a nonequilibrium process. The second law of thermodynamics guarantees that an equally weighted average of the work will yield a result larger than the free-energy difference. But Jarzynski showed that when the average taken over an infinite number of trials is Boltzmann-weighted according to the work required for each repetition, the result will always be the free-energy difference $\Delta F$. This relation holds even for processes arbitrarily far from equilibrium.

Liphardt *et al*. (*2*) tested Jarzynski's equality by comparing the work performed in the reversible and irreversible mechanical unfolding of a single RNA molecule. They performed a delicate experiment in which small beads were attached to the ends of a single strand of RNA. The bead at one end was held in an optical trap, which allowed the force (and, thus, by integration, the work) to be measured. The bead at the other end was held by a micropipette attached to a piezoelectric device, allowing the position of this bead to be controlled by changing the voltage in the device. The position $z$ of the second bead relative to an arbitrary position—a measure of the extent that the molecule has been unfolded—was used as the sole control parameter, giving a one-dimensional free-energy landscape as a function of $z$.

The researchers performed alternating trials of slower pulls (the quasi-reversible case) and pulls that were an order of magnitude faster (the nonequilibrium case). They found that the slower pulls were indeed approximately reversible. Repeated measurements yielded almost a single curve of work as a function of position $z$ of the second bead (shown schematically in the figure as a dashed blue line). For faster pulling speeds, the work required to unfold the molecule as a function of $z$ varied widely from trial to trial (solid red lines). The molecule does not have time to equilibrate during pulling, and the amount of work required therefore depends on the detailed microscopic configuration of the molecule. Small differences grow as the molecule is pulled at a nonreversible rate that prevents the various trials from settling into the common, equilibrium state.

Some individual trials actually require less work than the reversible case, but the majority require more work. In agreement with the second law of thermodynamics, the equally weighted average (dotted black line) is always larger than the reversible work. But when Liphardt *et al*. applied the weighting of the trials prescribed by Jarzynski, they found that the weighted average (dotted green line) agreed to within experimental error with the reversible work. Their results provide the first experimental demonstration that Jarzynski's equality is valuable not only as a theoretical construct but also as a practical (albeit technically challenging) method for mapping out free energy landscapes.

The Jarzynski equality is one of only a small number of relations between equilibrium properties and measurements made arbitrarily far from equilibrium, despite the prevalence of far-from-equilibrium processes in everyday life. As more relations are discovered or new uses of the known relations are developed [see for example (*6*)], we will continue to move closer to an understanding of these important and complicated nonequilibrium systems.

**References**

1. L. D. Landau, E. M. Lifshitz, *Statistical Physics* (Butterworth-Heinemann, Oxford, ed. 3, 1980).
2. J. Liphardt, S. Dumont, S. B. Smith, I. Tinoco Jr., C. Bustamante, *Science* **296**, 1832 (2002).
3. C. Jarzynski, *Phys. Rev. Lett.* **78**, 2690 (1997).
4. _____, *Phys. Rev. E.* **56**, 5018 (1997).
5. H. Frauenfelder, *Proc. Natl. Acad. Sci. U.S.A.* **99**, 2479 (2002).
6. B. Isralewitz, M. Gao, K. Schulten, *Curr. Opin. Struct. Biol.* **11**, 224 (2001).

PERSPECTIVES: IMMUNOLOGY

# T Cell Activation in Six Dimensions

**Ulrich H. von Andrian**

Immunologists are elucidating how the immune systems of higher animals retain specific memories of antigens that they have encountered in the past. A central player in the maintenance of immunological memory is the T lymphocyte, which originates in the thymus as a thymocyte. Thymocytes must assemble T cell receptors (TCRs) that recognize self major histocompatibility complex (MHC) molecules but not the self antigens that the MHC presents. Those thymocytes whose TCRs do not match these positive and negative selection criteria are eliminated.

T cells that survive thymic selection enter the bloodstream as so-called naïve T cells and begin a restless survey of the body for antigens that can stimulate their TCRs. For T cell activation to occur, antigen must be encountered in the context of both self MHC and costimulatory molecules on mature dendritic cells (DCs), which reside in organized lymphoid tissues such as lymph nodes. After leaving the thymus, naïve T cells continuously recirculate between the blood and lymphoid organs but do not enter other tissues (*1*, *2*). The critical events in this homing process—in particular, the adhesive and signaling interactions between circulating T cells and vascular endothelial cells—are well characterized. However, what happens to T cells in the thymus before their entry into the blood, and then after they exit the circulation and enter the lymph nodes, remains a mystery. Three elegant fluorescence microscopy studies reported in this issue shed new light, quite literally, on the dynamics and topography of T cells in living lymph nodes (*3*, *4*) and in thymic organ cultures (*5*).

Miller *et al*. on page 1869 (*3*) and Stoll *et al*. on page 1873 (*4*) image fluorescently labeled T cells in explanted mouse lymph nodes. Given that these lentil-shaped organs measure ~1 mm in diameter, these studies are a technical tour de force. Normal lymph nodes have several distinct layers: They are covered by a fibrous capsule, which encloses the subcapsular sinus, a

The author is at the Center for Blood Research, Department of Pathology, Harvard Medical School, Boston, MA 02115, USA. E-mail: uva@cbr.med.harvard.edu

lymph fluid–filled compartment; underneath this is the cortex, a layer that is rich in B cells and macrophages (see the figure). Most of the T cell compartment is localized in the subcortex several tens to hundreds of micrometers below the surface. To visualize T cells in this layer, both groups resorted to sophisticated microscopy that extracts visual information from deep within living tissue.

Stoll and colleagues used laser scanning confocal microscopy, which allowed them to generate time-lapse movies of fluorescent T cells migrating at a depth of up to 80 μm below the surface of the lymph node (*4*). At various times before lymph node harvesting, mice were injected with green fluorescent T lymphocytes intravenously, and red fluorescent DCs intradermally. Lymphocytes injected into the blood homed straight to the lymph nodes. In contrast, DCs entered local lymph vessels that channel interstitial fluid and cells from the skin to the local lymph node. Once the DCs had made their way to this skin draining lymph node, the organ was excised, incubated in an observation chamber, and microscopically viewed through appropriate fluorescent filters, which allowed the two cell populations to be followed in space and time.

When T helper cells initially encountered antigen-pulsed DCs in this system, they formed long-lived contacts with DCs, usually in a 1:1 ratio. At >37 hours after stimulation with antigen, T cells began to express activation markers, became dissociated from DCs, migrated more rapidly (at speeds of 5 to 7 μm/min), and started to divide (*4*). In an elegant experiment, the authors visualized the contact zone between T cells and antigen-bearing DCs. It has been established that surface molecules in this area become organized in a so-called supramolecular adhesion cluster or immunological synapse, with TCRs and costimulatory molecules concentrated in the center, surrounded by a circular region that is enriched in the adhesion molecule LFA-1 (*6*, *7*). In contrast, large negatively charged surface molecules, such as CD43, which may exert anti-adhesive effects (*8*), are excluded from this contact zone. This phenomenon is well documented in vitro, but it is not clear whether immunological synapses also form in vivo and whether they are necessary for T cell activation. In one study, interactions between T cells and DCs in a collagen matrix were highly dynamic, leading to efficient T cell activation despite an average T cell–DC contact time that was too short for the formation of a mature synapse (*9*). Stoll *et al.* (*4*) now report that these interactions last for many hours in lymph nodes, leaving ample time for immunological synapses to form. Consistent with this notion, they observed that CD43 on the T cell surface was excluded from the DC contact site.

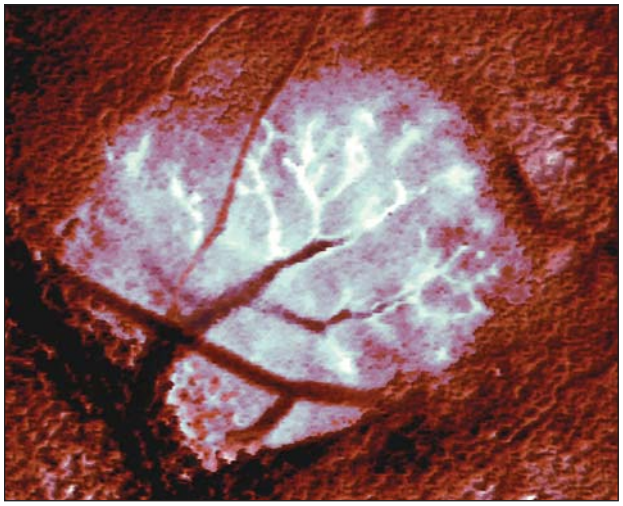

**Mysteries of the deep.** False-color micrograph of a lymph node in a living mouse stained with an intravital dye. The brown/orange material in the periphery is fatty tissue, which partially covers the lymph node (purple/blue). High endothelial venules (white) are the entry point for lymphocytes homing to the lymph nodes from the circulation. They were labeled with a fluorescein-tagged monoclonal antibody that recognizes the lymph node–specific adhesion molecule addressin (PNAd).

Miller *et al*. (*3*) address many of the same questions, but with notable differences in technique resulting in somewhat different findings. Like Stoll and colleagues, Miller *et al*. also performed adoptive transfer of fluorescently tagged murine lymphocytes and then observed homing of the cells in explanted lymph nodes. However, these authors used real-time two-photon laser microscopy instead of single-photon confocal microscopy. This technique allows deeper imaging into the T cell area of the lymph node (up to 350 μm beneath the surface). It also results in lower phototoxicity and less photobleaching of fluorophores because, unlike single-photon confocal excitation, fluorescence excitation is limited to a volume of ~1 $\mu m^3$ surrounding the focal point of the microscope objective (*10*). Like Stoll *et al*., Miller *et al*. found that T cells moved randomly without pursuing any apparent direction for long periods, but they report higher migration speeds (up to 25 μm/min) even in the absence of antigen (*3*).

To assess the effects of antigenic challenge on T cell behavior, Miller *et al*. used ovalbumin as a model antigen, which they injected in an alum emulsion together with tumor necrosis factor–α as an adjuvant (*3*). Unlike injection of in vitro generated antigen-pulsed DCs (*4*), this approach relies on endogenous DCs at the injection site to process the antigen and carry it to the draining lymph node. T cell behavior in response to this challenge was notably different from that observed by Stoll and co-workers. After 1 day, some T cells were found in relatively stationary clusters, whereas others were described as "'swarms,' looping within regions a few tens of μm across" (*3*). Miller *et al*. did not attempt to visualize antigen-presenting cells in their experiments, but it seems likely that both clusters and local swarms of T cells may have colocalized with DCs. Interestingly, although more stationary T cells were observed by Miller *et al*. upon antigenic challenge, these cells were in the minority. In contrast, long-lived stationary interactions between T cells and antigen-presenting DCs were the norm in the Stoll *et al*. work (*4*). Moreover, subcutaneously injected antigen-laden DCs appeared to interact with just one T cell in lymph nodes (*4*), whereas the presence of T cell swarms and clusters in response to soluble protein antigen injection suggests a higher T cell:DC ratio (*3*). Although these behavioral differences remain to be explained, the more dynamic appearance of T cells in the Miller *et al*. work raises new questions about the physiological importance of immunological synapse formation to T cell activation.

These two reports raise several other questions. Most important, lymph nodes had to be removed from animals for observation. Thus, the organs were deprived of physiologic input via the blood, afferent lymph, and peripheral nerves. Lymph flow, in particular, can have a modulating effect on lymph node homeostasis. Interruption of afferent lymphatics in vivo leads to rapid loss of normal lymphocyte traffic (*11*, *12*). The lymph is also a conduit through which chemokines are channeled into lymph nodes (*13*–*15*). Lymphocytes sense concentration gradients of chemokines and migrate toward them (*16*). It is conceivable that lymph flow is necessary to maintain labile chemokine gradients, which might guide migrating T cells in a more directed fashion than the random motion observed in the excised lymph nodes. Another technical issue is the maintenance of physiologic gas exchange in unperfused lymph nodes. In metabolically active tissues, normoxic blood flow maintains sufficient tissue oxy-

genation up to a distance of <200 μm from the closest capillary (*17*). Because gas exchange in explanted lymph nodes must occur exclusively across the surface capsule, it is likely that a steep gradient in tissue oxygen tension was established, with the lowest concentration being in the deep T cell area. Miller *et al*. used a 95% $O_2$ gas mixture in their incubation chamber (*3*), whereas Stoll *et al*. used 20% $O_2$ (*4*). Whether and to what extent differences in methodology between the two studies might account for disparities in T cell behavior remains to be determined.

Although two-photon microscopy is used routinely for intravital imaging of living cells and solid tissues, especially in neurobiology and embryology (*18*, *19*), it has found surprisingly little application among immunologists (*3*, *20*). This situation is set to change with the new reports because the technology is clearly admirably suited for addressing many important immunological questions. For example, the Bousso *et al*. study on page 1876 of this issue (*5*) opens a new frontier in immunological imaging by using two-photon microscopy to observe how thymocytes run the gauntlet of positive selection in three-dimensional thymic organ cultures. As observed with mature T cells in lymph nodes (*3*, *4*), engagement of thymocyte TCRs with self antigen presented (in the context of MHC) by thymic stromal cells enhanced the dynamics and duration of T cell–stromal cell contacts (*5*). It will be important to dissect the signals that govern these striking changes in cellular behavior and to determine how these events shape cellular immune responses both inside and outside the thymus. Undoubtedly, six-dimensional imaging strategies that measure the light intensity, color, and motion in space and time of single immune cells in living tissues (and ideally in live animals) will be a critical tool for probing ever more deeply into the mysteries of immunity.


**References**

1. E. C. Butcher, L. J. Picker, *Science* **272**, 60 (1996).
2. U. H. von Andrian, C. R. Mackay, *N. Engl. J. Med.* **343**, 1020 (2000).
3. M. J. Miller, S. H. Wei, I. Parker, M. D. Cahalan, *Science* **296**, 1869 (2002); published online 16 May 2002 (10.1126/science.1070051).
4. S. Stoll, J. Delon, T. M. Brotz, R. N. Germain, *Science* **296**, 1873 (2002).
5. P. Bousso, N. R. Bhakta, R. S. Lewis, E. Robey, *Science* **296**, 1876 (2002).
6. C. R. F. Monks *et al*., *Nature* **395**, 82 (1998).
7. A. Grakoui *et al*., *Science* **285**, 221 (1999).
8. N. Manjunath *et al*., *Nature* **377**, 535 (1995).
9. M. Gunzer *et al*., *Immunity* **13**, 323 (2000).
10. W. Denk *et al*., *Science* **248**, 73 (1990).
11. H. R. Hendriks *et al*., *Eur. J. Immunol.* **17**, 1691 (1987).
12. R. E. Mebius *et al*., *J. Cell Biol.* **115**, 85 (1991).
13. J. V. Stein *et al*., *J. Exp. Med.* **191**, 61 (2000).
14. J. E. Gretz *et al*., *J. Exp. Med.* **192**, 1425 (2000).
15. R. T. Palframan *et al*., *J. Exp. Med.* **194**, 1361 (2001).
16. C. R. Mackay, *Nature Immunol.* **2**, 95 (2001).
17. I. P. Torres Filho *et al*., *Proc. Natl. Acad. Sci. U.S.A.* **91**, 2081 (1994).
18. F. Helmchen *et al*., *Neuron* **31**, 903 (2001).
19. P. T. So *et al*., *Annu. Rev. Biomed. Eng.* **2**, 399 (2000).
20. C. C. Norbury *et al*., *Nature Immunol.* **3**, 265 (2002).


PERSPECTIVES: NEUROSCIENCE

# Neurons in Action

**Peter König and Paul F. M. J. Verschure**

Much of brain research is fueled by the wish to unravel the foundations of thought and action (*1*). Whereas the complex neural processes that underlie consciousness are beginning to be elucidated, the simpler neural circuitry that drives perception and the generation of movement surprisingly remains unclear. For instance, we still do not know whether movement depends on a few localized neuronal circuits or the dynamic state of multiple distributed neuronal systems. Much of the hope surrounding neuroprosthetic devices that translate the activity of neurons in the brain into muscle movements depends on understanding how neurons normally initiate and control skeletal muscles. Toward this goal, work by Taylor *et al.* (*2*) on page 1829 of this issue reveals that the activity of a small group of motor cortex neurons in monkeys can be fine-tuned to carry out complex three-dimensional (3D) movements.

Much of our knowledge about neurons has come from studies of the neuromuscular junction, the point where nerve and muscle meet (*3*, *4*). When parts of the motor system are damaged through injury or disease, repair efforts concentrate on trying to restore the link between neuronal activity and muscle contraction. There have been attempts to achieve this using noninvasive methods, such as electroencephalography (*5*). In this case, recording of the bulk signal of millions of neurons in the motor cortex is analyzed online, resulting in information rates of up to 1 bit/second that can be harnessed to control real-world devices that, for example, dial the phone or switch on the heating.

However, in order to restore speed and fluidity to the motor system, the activity of more neurons needs to be commandeered. The question of exactly how many neurons is crucial for understanding cortical representations of movement in the brain. Experiments using single-neuron electrode recordings in monkeys as they perform a reaching task suggest that movement depends on activation of millions of neurons in a wide area of the motor cortex (*6*). Each neuron in the motor cortex is maximally active for a particular direction of movement, but also fires to a lesser degree in response to movements in other directions. The average of the preferred move-

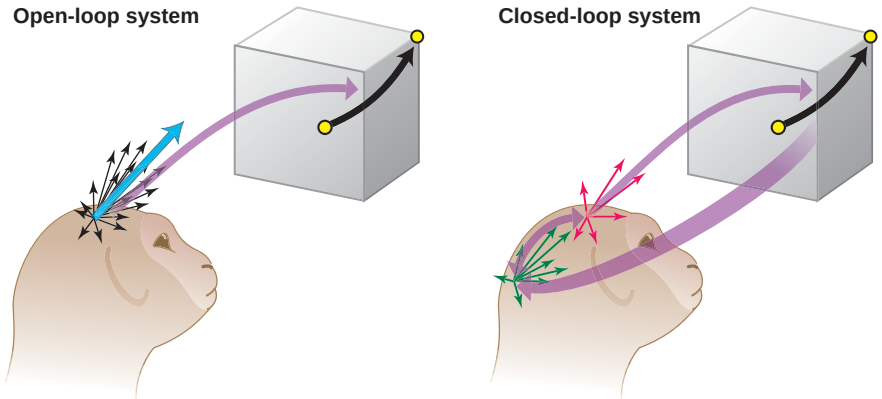


**Think local.** Movement of a cursor (yellow sphere) directed by the activity of cortical neurons in the monkey brain. (**Left**) In an open-loop experiment, the preferred direction of movement of a large number of neurons and the weighted average activity of each neuron determines the direction of cursor movement (blue arrow). (**Right**) In a closed-loop experiment (*2*), visual feedback (green arrows) results in adaptation of a small group of motor cortex neurons (red arrows), which are sufficient to accurately control cursor movement. Mapping of the visual cortex onto the motor cortex, and of the motor cortex onto the action performed, is adaptable and can be fine-tuned through learning and visual feedback.

The authors are at the Institute of Neuroinformatics, University/ETH Zürich, Winterthurerstrasse 190, 8057 Zürich, Switzerland. E-mail: peterk@ini.phys.ethz.ch, pfmjv@ini.phys.ethz.ch